Journal of Chromatography A, 1581–1582 (2018) 100–104

Contents lists available at ScienceDirect

Journal of Chromatography A

journal homepage: www.elsevier.com/locate/chroma

Flow optimisations with increased channel thickness in asymmetrical flow field-flow fractionation

Joon Seon Yang, Myeong Hee Moon*

Department of Chemistry, Yonsei University, 50 Yonsei-ro, Seoul, 03722, South Korea

ARTICLE INFO

Article history:
Received 14 May 2018
Received in revised form 26 October 2018
Accepted 29 October 2018
Available online 31 October 2018

Keywords:
Asymmetrical flow field-flow fractionation
Channel thickness effect
Resolution
Protein separation

ABSTRACT

Retention in flow field-flow fractionation (flow FFF) is generally governed by the combination of crossflow and migration flowrates. Especially for an asymmetrical flow FFF (AF4) channel in which the channel-inlet flow is divided into crossflow and outflow, the separation of low-molecular-weight proteins or macromolecules requires a relatively high crossflow rate along with a very low outflow rate for a reasonable level of resolution, which often leads to a limitation in channel pressure. In this study, the performances of AF4 with increased channel thicknesses have been investigated by adjusting the effective channel flowrates in the asymmetrical channels according to the variation of channel thickness. Four AF4 channels of different channel thicknesses (350, 490, 600, and 740 μm) were employed to examine the potential usefulness of employing a thick channel in the high-resolution separation of low-molecular-weight proteins (< 100 kDa) and to determine the relationship between higher channel thickness and the recovery of elution. Experiments showed that the ratio of crossflow rate to the effective channel flowrate should be considered in the selection of a run condition at an increased channel thickness. The study also demonstrated that a thick AF4 channel can be useful for the high-resolution separation of low-molecular-weight species such as protein aggregates without using extremely high crossflow rates.

1. Introduction

Flow field-flow fractionation (flow FFF), a variant of the FFF family, is an elution-based separation method capable of fractionating particles and macromolecules by size [1–4]. Separation in flow FFF is carried out in a thin empty channel space without a stationary phase by applying two flow streams moving perpendicular to each other: a channel flow, which drives the sample components towards the end of a channel, and a crossflow, which moves across the channel wall to force the migrating sample components towards the accumulation wall. As the flow profile in a thin channel becomes parabolic, where the flow velocity becomes the lowest near the channel wall and maximum at the centre across the channel thickness, particles or macromolecules with a small diameter protrude further away from the wall as their diffusion is faster than that of components with large diameters. Therefore, the smaller components elute earlier than the larger ones. As flow FFF can utilise aqueous solutions including a biological buffer as the carrier liquid, it has been applied to various biological materials including proteins and protein aggregates [5,6], DNA [7], microRNA [8], plasma lipoproteins [9], exosomes [10,11], subcellular species [12], cells [13,14], virus-like particles [15], and water-soluble polymers [16,17].

Retention in flow FFF is affected by two important parameters: the rates of crossflow (external field strength) and channel flow [18], once other experimental factors such as the compatibility of sample components with the carrier solution and the type of channel membrane materials are assured. In a symmetrical flow FFF channel, which utilises two permeable frits at both channel walls (depletion and accumulation walls), channel flowrate (axial flowrate) remains the same throughout the channel and is equal to the outflow rate; therefore, the retention time is determined by the ratio of outflow rate to crossflow rate for a given channel thickness. Generally, the separation resolution can be improved by increasing crossflow rate, however it results in the increase in the analysis time. Consequently, a simultaneous increase in crossflow and outflow rates leads to a speedy analysis without loss of resolution. However, an increase in both flowrates often leads to a limitation in the channel pressure, which may lead to a leaking problem. In the case of an asymmetrical flow FFF (AF4) channel, only one permeable frit is utilised at the accumulation wall by replacing the permeable depletion wall with a solid impermeable block. Therefore, part of the flow entering the channel inlet is divided into crossflow and the remaining exits as outflow, and hence, the transport of the

* Corresponding author.
E-mail address: mhmoon@yonsei.ac.kr (M.H. Moon).

https://doi.org/10.1016/j.chroma.2018.10.053
0021-9673/

carrier liquid or channel flow is reduced along the channel axis. As a simple increase in the crossflow rate of AF4 accompanies the simultaneous increase in the axial flow along the channel axis, the outflow rate should be adjusted to be as low as possible (~ a few tenths of 1 mL/min) with a sufficiently high crossflow rate to obtain a reasonable level of resolution for separation. Typically, for the separation of low-MW (MW: molecular weight) species such as proteins, a channel spacer with a reduced thickness (< 250 μm) offers high-resolution separation by using a high crossflow rate. Experimentally, it requires a careful selection of both crossflow and outflow rates. To increase the separation resolution of sample components with low MW, a very high rate of channel inlet flow should be introduced to maintain a high crossflow rate, which incurs the limitation of both channel pressure and pump system.

This study investigated ways to maintain or improve the resolution of separation in AF4 channels by increasing the channel thickness while examining the roles of crossflow rate and effective channel flowrate. AF4 channels of four different thicknesses (350, 490, 600, and 740 μm) were employed to examine the potential use of a thick channel for protein separation with an improved resolution instead of using a thin channel, which normally requires a high channel inlet flowrate. Focused were on the optimisation of flowrate conditions in AF4 by varying the channel thickness and the investigation of the peak recovery in channels of increased thicknesses at different field strengths. This study also demonstrated the usefulness of employing a thick channel in AF4 for the high-resolution separation of protein aggregates.

2. Theory

The retention ratio, R, in FFF is defined as the ratio of channel void time, t°, to retention time, t_r, and is simply expressed as

$$R = \frac{t^0}{t_r} = \frac{2kT}{\pi\eta w U d} \tag{1}$$

where kT is the thermal energy, η is the viscosity of the carrier liquid, w is the channel thickness, U is the transverse velocity of sample components across the channel driven by an external field, and d is the particle diameter [1,2]. In the case of flow FFF, U becomes the transverse velocity of crossflow represented as $\dot{V}_c/bL$ where $\dot{V}_c$ is the crossflow rate, b is the channel breadth, and L is the channel length; therefore, the retention time of a sample component in flow FFF can be theoretically predicted with a good estimation of channel void time and crossflow rate as

$$t_r = \frac{\pi\eta w d \dot{V}_c}{2kTbL} t^0 \tag{2}$$

The calculation of void time in flow FFF depends on the type of channel system (i.e. symmetrical, asymmetrical, and cylindrical channel). t° in a symmetrical flow FFF channel is expressed as $V^0/\dot{V}$, which is the passage time of a non-retained component through the channel volume ($V^\circ = bwL$) at a migration flowrate ($\dot{V}$). Thus, Eq. (2) becomes

$$t_r = \frac{\pi\eta w^2 d}{2kTbL}\frac{\dot{V}_c}{\dot{V}} \text{ (for a symmetrical channel)} \tag{3}$$

However, in an asymmetrical flow FFF (AF4) channel, void time is expressed as [3,19]

$$t^0 = \frac{V^0}{\dot{V}_c}\ln\left(\frac{\dot{V}_{in} - \frac{A(z)}{A_c}\dot{V}_c}{\dot{V}_{out}}\right) \tag{4}$$

where $\dot{V}_{in}$ and $\dot{V}_{out}$ are the volumetric flowrates of the channel inlet and outlet, respectively, A_c is the total area of the accumulation wall, and A(z) is the area of the accumulation wall from the channel inlet up to distance z from the inlet, typically at the focusing/relaxation point. By a comparison with the void time in a symmetrical channel ($= V^0/\dot{V}$), the effective migration flowrate, $\dot{V}_{eff}$, in an asymmetrical channel system can be expressed as

$$\dot{V}_{eff} = \dot{V}_c\left[\ln\left(\frac{\dot{V}_{in} - \frac{A(z)}{A_c}\dot{V}_c}{\dot{V}_{out}}\right)\right]^{-1} \text{ (for an asymmetrical channel)} \tag{5}$$

Thus, the retention time in flow FFF is generally expressed, regardless of the channel type, as follows:

$$t_r = \frac{\pi\eta w^2 d}{2kTbL}\frac{\dot{V}_c}{\dot{V}_{eff}} \tag{6}$$

Eq. (6) is generally applied to both channel systems of flow FFF in which $\dot{V}_{eff}$ becomes $\dot{V}_{out}$ for a symmetrical channel system and the ratio $\dot{V}_c/\dot{V}_{eff}$ for an asymmetrical channel system becomes

$$\frac{\dot{V}_c}{\dot{V}_{eff}} = \ln\left(\frac{\dot{V}_{in} - \frac{A(z)}{A_c}\dot{V}_c}{\dot{V}_{out}}\right) \tag{7}$$

Eq. (7) can be utilised to optimise the run condition of AF4 when the channel thickness is varied. By reducing the ratio $\dot{V}_c/\dot{V}_{eff}$ with an increase in channel thickness (as they are inversely proportional to each other in Eq. (6)), the retention time of a sample component can be synchronised at different channel thicknesses when the resolution of separation is maintained.

3. Experimental

Eight protein standards were purchased from Sigma–Aldrich (St. Louis, MO, USA): ferredoxin (11 kDa), myoglobin (17 kDa), carbonic anhydrase (CA, 29 kDa), α-1 acid glycoprotein (AGP, 41 kDa) from human, ovalbumin (OVA, 43 kDa), bovine serum albumin (BSA, 66 kDa), transferrin (78 kDa), and alcohol dehydrogenase (AD, 150 kDa). An AF4 channel (model LC) from Wyatt Technology Europe GmbH (Dernbach, Germany) was utilised with the regenerated cellulose membrane (MWCO 10 kDa) from Merck Millipore (Darmstadt, Germany). A same channel membrane was used throughout the experiments once flow optimizations were achieved. The channel membrane was cleaned at the end of a run by pumping channel flow at 4 mL/min for at least 5 min. without applying the crossflow rate. When replacing the channel spacer, the membrane was cleaned by gently rinsing the surface with deionized water. Channel spacers of three different thicknesses (250, 350, and 490 μm) were used in combination to assemble channels of thicknesses 600 and 740 μm. All the channels had a trapezoidal design: tip-to-tip channel length of 26.7 cm, inlet breadth of 2.1 cm, and final breadth of 0.5 cm. The lengths of both triangular end-pieces of a channel were 2.0 and 0.6 cm for the inlet and outlet triangles, respectively. Sample components were injected into the channel using a model 7125 injector from Rheodyne (Cotati, CA, USA) with a sample loop (25 μL) in the focusing/relaxation mode, and the injected sample materials were focused at the 1/10 position (z = 2.7 cm) from the channel inlet with the total flowrate of 3.0 mL/min for 1.5 min. All of the samples were reconstituted in a PBS buffer at a concentration of 0.1 mg/mL for each protein and the injection amount was 2.5 μg for each. AF4 experiments were carried out at isocratic field strength conditions. The carrier solution for AF4 was 0.1 M phosphate-buffered saline (PBS) solution (pH 7.4, 137 mM NaCl, 2.7 mM KCl, 10 mM Na_2HPO_4, and 1.7 mM KH_2PO_4) with 0.02% NaN_3 as bactericide prepared using ultrapure water (> 18 MΩ•cm) and filtered through a nitrocellulose filter (pore size = 0.22 μm) from Millipore prior to use. The carrier solution was delivered using a model SP930D HPLC pump from Young-Lin Instruments (Seoul, Korea) and the eluted sample components were monitored at 280 nm using a model YL9120 UV–vis detector

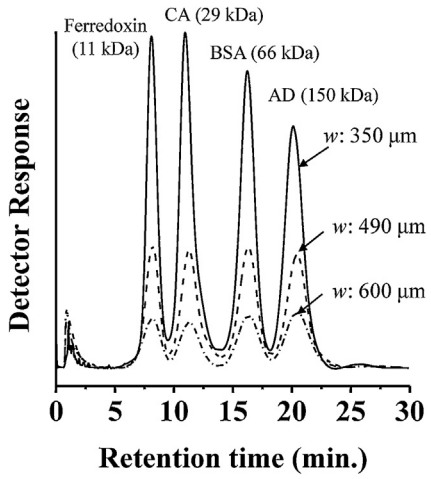

Fig. 1. AF4 separation of four protein standards (ferredoxin, CA: carbonic anhydrase, BSA: bovine serum albumin, and AD: alcohol dehydrogenase) at three channels of different thicknesses (w: 350, 490, and 600 μm), showing the synchronised retention time by adjusting $\dot{V}_c/\dot{V}_{eff}$ ratio according to the increase in channel thickness. Flowrate conditions were $\dot{V}_{in}$:$\dot{V}_{out}$ = 7.00:0.17 (w: 350 μm), 3.80:0.64 (w: 490 μm), and 3.00:0.90 (w: 600 μm). Injection amount for each protein standard was 2.5 μg. $\dot{V}_c/\dot{V}_{eff}$ ratios were 3.60, 1.67, and 1.12 in the increasing order of channel thickness.

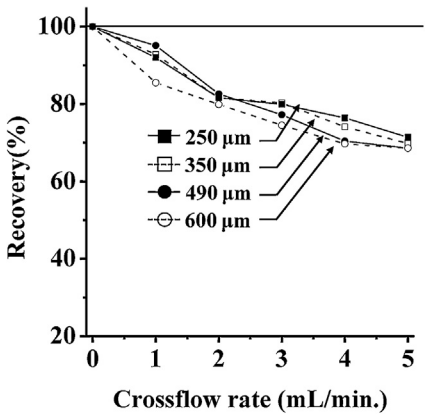

Fig. 2. Effect of crossflow rate on the peak recovery of BSA at a fixed outflow rate ($\dot{V}_{out}$ = 1.0 mL/min) using AF4 channels of different thicknesses.

from Young-Lin Instruments. The detector signals were recorded using Autochro 3000 software from Young-Lin.

4. Results and discussion

Four different channel spacers with thicknesses of 350, 490, 600, and 740 μm were utilised in this study, and the actual thickness of each channel system was calculated as 320, 467, 571, and 702 μm, respectively, from the theory (Eq. 6) using the experimental retention time of BSA obtained at $\dot{V}_{in} : \dot{V}_{out} = 7.76 : 0.76$. Based on the calculated values of channel thickness, separation of the four protein standards (ferredoxin, CA, BSA and AD) was accomplished by decreasing the $\dot{V}_c/\dot{V}_{eff}$ ratio according to the increase in channel thickness in Eq. (6). In the 350-μm-thick channel, protein separation was accomplished using the flowrate condition $\dot{V}_{in} : \dot{V}_{out} = 7.0 : 0.17$ ($\dot{V}_c/\dot{V}_{eff}$ = 3.60). The flowrates were varied to $\dot{V}_{in} : \dot{V}_{out}$ = 3.80:0.64 ($\dot{V}_c/\dot{V}_{eff}$ = 1.69) and 3.00:0.90 ($\dot{V}_c/\dot{V}_{eff}$ = 1.12) for the 490- and 600-μm-thick channels, respectively. Fig. 1 shows the superimposed fractograms of the four protein standard mixtures obtained with the three different channels, indicating that the retention time of each component was approximately the same in different channels. The reduction in the detector signals with the increase in channel thickness originated from the dilution of eluting components caused by the increase in detector flowrate (or $\dot{V}_{out}$). Fig. 1 confirms that the separation was maintained in thicker channels without losing resolution and the separation speed by varying the $\dot{V}_c/\dot{V}_{eff}$ ratio. The recovery of sample components in thicker channels was examined using BSA by varying the crossflow rate at a fixed outflow rate of 1.0 mL/min as shown in Fig. 2. The recovery in FFF may typically decrease with the increase in field strength and the decrease in outflow rate. The recovery values of BSA in this study were determined to be 92–71% at crossflow rates ranging from 1.0 to 5.0 mL/min for the 250-μm-thick channel in Fig. 2, which are very close to those reported in an earlier work [20]. The recovery values in the channels with increased thicknesses 490 and 600 μm decreased to some degree (< 5%) as shown in Fig. 2; however, they were not significantly reduced. In general, separation in a thin channel (< 250 μm) often requires the use of a high crossflow rate together with a low outflow rate. However, use of a low outflow rate ($\dot{V}_{out}$ = 0.2 mL/min) in a previous study resulted in a further decrease in recovery to ~50% level [19]. However, when using a thicker channel, a low crossflow rate can be employed along with a relatively high outflow rate without the loss of separation speed and resolution to achieve sample recovery.

The influence of $\dot{V}_c/\dot{V}_{eff}$ on the separation in AF4 with a thick channel (w = 490 μm) is demonstrated in Fig. 3 by varying either $\dot{V}_{eff}$ alone or the $\dot{V}_c/\dot{V}_{eff}$ ratio with the separation of seven protein standards: ferredoxin (11 kDa), myoglobin (17 kDa), carbonic anhydrase (29 kDa), ovalbumin (43 kDa), α-1 acid glycoprotein (41 kDa), transferrin (78 kDa), and alcohol dehydrogenase (AD, 150 kDa). In general, the efficiency of separation in an FFF system is enhanced by increasing the field strength. However, in an AF4 channel system whose $\dot{V}_{eff}$ increases with an increase in crossflow rate, the selection of a run condition should be considered with the ratio of $\dot{V}_c/\dot{V}_{eff}$. Fig. 3a shows the separation of seven proteins achieved at $\dot{V}_{in}$:$\dot{V}_{out}$ = 7.0:2.0 ($\dot{V}_{eff}$ = 4.26 mL/min, $\dot{V}_c/\dot{V}_{eff}$ = 1.17). Owing to a relatively low ratio of $\dot{V}_c/\dot{V}_{eff}$ = 1.17, even with a high $\dot{V}_{eff}$ = 4.26 mL/min, a poor separation was achieved. By reducing the outflow rate, $\dot{V}_{out}$, to 1.0 mL/min with the crossflow rate fixed at 5.0 mL/min in the run b, the retention times of all the components were prolonged and the resolution was improved. In this case, $\dot{V}_{eff}$ was reduced to 2.94 mL/min and $\dot{V}_c/\dot{V}_{eff}$ was increased to 1.70. Instead of reducing $\dot{V}_{out}$, $\dot{V}_{in}$ was maintained the same as that in the run a (7.0 mL/min) and flowrates were adjusted to $\dot{V}_{in}$:$\dot{V}_{out}$ = 7.0:1.16 so that $\dot{V}_{eff}$ was adjusted to 3.42 mL/min in the run c, which shows a similar result as in the run b. However, when $\dot{V}_c/\dot{V}_{eff}$ was further increased to 2.12 in the run d ($\dot{V}_{in}$:$\dot{V}_{out}$ = 7.0:0.76) without altering $\dot{V}_{eff}$, the resolution of separation was further improved. From the runs c and d in Fig. 3, it can be observed that the efficiency of separation in AF4 is dependent on the proper control of $\dot{V}_c/\dot{V}_{eff}$. Under the same flowrate conditions in Fig. 3d, the same protein mixtures were further tested at increased channel thicknesses (w = 600 and 740 μm) in Fig. 4, indicating that all the components were nearly resolved at the baseline level in both channels, except ovalbumin and AGP, whereas the retention times were substantially increased owing to the increase in channel thickness. The retention times of proteins are plotted in the logarithmic scale against the Stoke's diameter of each species found in literature in Fig. 5 along with the comparison with the theoretically expected time (solid line), indicating that protein species eluted slightly earlier than expected but the differences were not significant. The retention times of AGP (third data point from the right) in the three channels appeared to be outside the linear relationship, based on the molar mass (41 kDa) of AGP provided by the manufacturer. If AGP used in this study were 41 kDa, it would elute with ovalbumin (43 kDa) owing to the very small difference in MWs. However, AGP appeared to elute later and the overlap of the two proteins was not significant as shown in Figs. 3 and 4, indicating

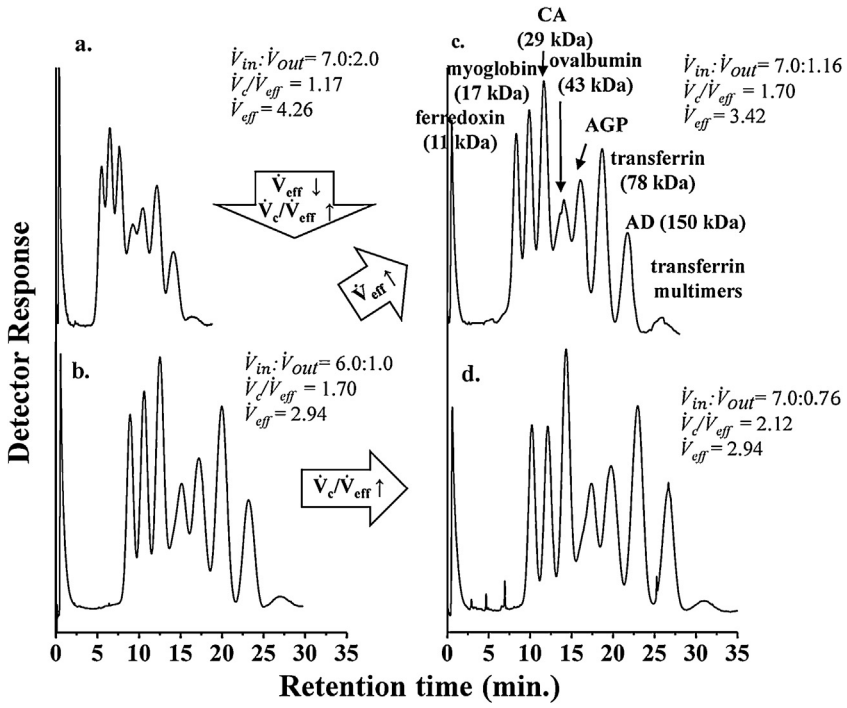

Fig. 3. Effects of $\dot{V}_c/\dot{V}_{eff}$ on the separation of a mixture of seven protein standard proteins (2.5 μg each) in a 490-μm-thick channel. $\dot{V}_{in}$ was 7.0 mL/min for the runs a, c, and d and 6.0 mL/min for b.

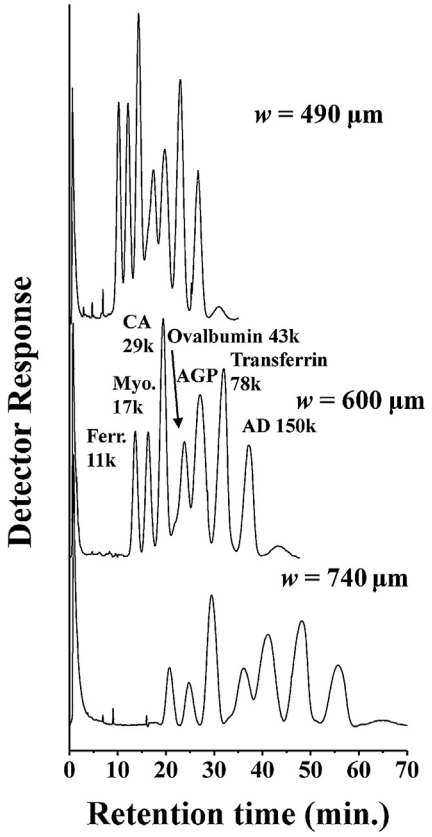

Fig. 4. AF4 separation of a mixture of seven protein standards by increasing the channel thickness (490, 600, and 740 μm) at a fixed run condition: $\dot{V}_{in}$:$\dot{V}_{out}$ = 7.00:0.76.

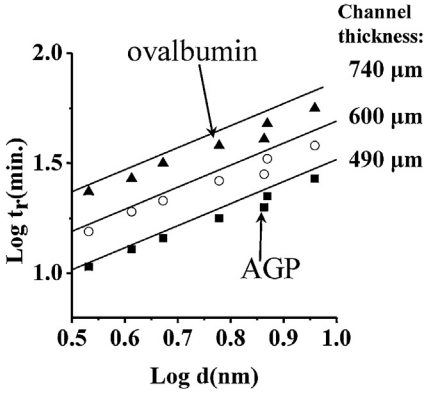

Fig. 5. Plots of log t_r vs. log d (Stoke's diameter) of protein standards (data points) at different channel thicknesses along with theoretical retention time (solid line).

that their MWs are not similar. AGP is known to contain approximately 45% of carbohydrates, and there are two forms of AGP (54 and 40 kDa) depending on the cleavage of sialic acid residues [21].

Therefore, we estimated the MW and Stoke's diameter of AGP by establishing calibration curves without including AGP data based on the data obtained with a 600-μm-thick channel. The calibration parameters were log t_r = 0.365 log MW – 0.4525 (R^2 = 0.991) and log t_r = 0.987 log d + 0.6317 (R^2 = 0.9962) for the calculation of MW and diameter, respectively, showing a good linearity in regression. From the calibration curves, the MW and Stoke's diameter of AGP were calculated to be 58.4 kDa and 6.5 nm, respectively. The calculated MW value was slightly higher than the reported value (54 kDa) of the larger form of AGP without the loss of sialic acid; however, the calculated diameter was similar to the known value (7.0 nm) [22]. Similarly, a small peak observed after the peak of AD in Figs. 3 and 4 was expected to be from the multimeric forms of transferrin, not from the aggregates of AD as shown in the fractograms obtained with the individual injections of transferrin and AD (not shown here). The MW value of the multimeric form calculated from its retention time with the above calibration parameters was approximately 202 kDa, larger than those of dimeric forms of transferrin.

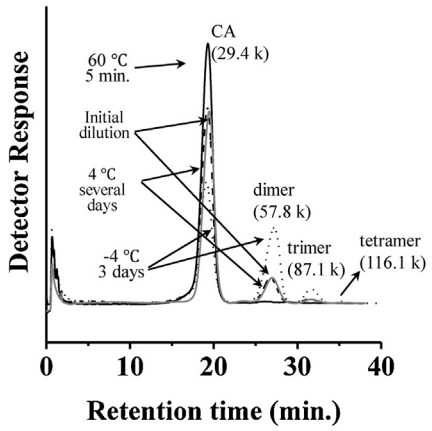

Fig. 6. Effect of temperature on the formation of aggregates of carbonic anhydrase in AF4 (w = 600 μm) obtained at $\dot{V}_{in}$:$\dot{V}_{out}$ = 7.00:0.76.

Finally, the capability of AF4 for the high-resolution separation of protein aggregates using an increased channel thickness (w = 600 μm) is demonstrated in Fig. 6 with CA (29.4 kDa). Fractograms of Fig. 6 show the baseline separation of CA and its multimers, which were stored at different temperatures. The flowrate conditions were the same as those used in Fig. 3d and the injection amount of CA was 10 μg for each injection. When dried form of CA was dissolved in the PBS buffer solution, it was run immediately (grey line) and after storage at 4 °C (short dash line) for a few days, dimers (58.8 kDa) and trimers (87.8 kDa) were observed from their isolated peaks. When it was frozen, stored at −4 ° (dotted line) for three days, and thawed, the intensity of the monomer peak was further decreased and those of the multimeric species increased. In this case, the tetrameric form was also detected. However, when the original solid CA species was dissolved in the buffer and warmed at 60 °C for 5 min (solid line), the multimer peaks disappeared and a substantial increase in the monomer peak was observed. The MW values of each multimeric species estimated from the calibration curve established above were 57.8, 87.1, and 116.1 kDa for the dimer, trimer, and tetramer, respectively. Fig. 6 shows that AF4 with a thicker channel can achieve high-resolution separation of proteins and their aggregates, which can be generated during storage at different temperatures, pH values, and salt concentrations.

5. Conclusion

In this study, the separation in an AF4 with thick channels was optimised by varying the effective channel flowrates in an asymmetrical channel. In the case of an AF4 channel system whose effective channel migration flowrate simultaneously increases with the crossflow, the ratio of crossflow rate to the effective channel flowrate should be considered for the selection of suitable conditions in order to achieve the desired resolution. To improve the resolution of separation, a decrease in the effective channel flowrate is to be considered prior to the increase in $\dot{V}c/\dot{V}eff$ for a given channel thickness. An AF4 system with a typically thin channel (< 250 μm) requires the use of a high crossflow rate with a low outflow rate for the high-resolution separation of low-MW proteins (< 100 kDa) and macromolecules, whereas separation with thicker channels can be useful to achieve an equivalent or higher-resolution separation at a reduced crossflow rate without incurring an unwanted interaction of sample components with a strong field strength, which is conducive to the minimizing possible sample loss. Moreover, once $\dot{V}c/\dot{V}eff$ ratio is properly selected, it is useful to achieve improved separation for low-MW proteins or macromolecules when using a thicker channel.

Acknowledgement

This study was supported by the grant NRF-2018R1A2A1A05019794 from the National Research Foundation (NRF) of Korea.

References

[1] J.C. Giddings, Field-Flow Fractionation: analysis of macromolecular, colloidal, and particulate materials, Science 260 (1993) 1456–1465.
[2] M.E. Schimpf, K.D. Caldwell, J.C. Giddings, Field-Flow Fractionation Handbook, Wiley Interscience, New York, 2000.
[3] K.-G. Wahlund, J.C. Giddings, Properties of an asymmetrical flow field-flow fractionation channel having one permeable wall, Anal. Chem. 59 (1987) 1332–1339.
[4] S.K. Ratanathanawongs, J.C. Giddings, Dual-field and flow-programmed lift hyperlayer field-flow fractionation, Anal. Chem. 64 (1992) 6–15.
[5] A. Hawe, W. Friess, M. Sutter, W. Jiskoot, Online fluorescent dye detection method for the characterization of immunoglobulin G aggregation by size exclusion chromatography and asymmetrical flow field flow fractionation, Anal. Biochem. 378 (2008) 115–122.
[6] P. Reschiglian, B. Roda, A. Zattoni, M. Tanase, V. Marassi, S. Serani, Hollow-fiber flow field-flow fractionation with multi-angle laser scattering detection for aggregation studies of therapeutic proteins, Anal. Bioanal. Chem. 406 (2014) 1619–1627.
[7] J. Ashby, S. Schachermeyer, Y. Duan, L.A. Jimenez, W. Zhong, Probing and quantifying DNA-protein interactions with asymmetrical flow field-flow fractionation, J. Chromatogr. A 1358 (2014) 217–224.
[8] J. Ashby, K. Flack, L.A. Jimenez, Y. Duan, A.K. Khatib, G. Somlo, S.E. Wang, X. Cui, W. Zhong, Distribution profiling of circulating microRNAs in serum, Anal. Chem. 86 (2014) 9343–9349.
[9] J.Y. Lee, S.K. Byeon, M.H. Moon, Profiling of oxidized phospholipids in lipoproteins from patients with coronary artery disease by hollow fiber flow field-flow fractionation and nanoflow liquid chromatography-tandem mass spectrometry, Anal. Chem. 87 (2015) 1266–1273.
[10] D. Kang, S. Oh, S.M. Ahn, B.H. Lee, M.H. Moon, Proteomic analysis of exosomes from human neural stem cells by flow field-flow fractionation and nanoflow liquid chromatography-tandem mass spectrometry, J. Proteome Res. 73 (2008) 3475–3480.
[11] S. Sitar, A. Kejžar, D. Pahovnik, K. Kogej, M. Tušek-Žnidarič, M. Lenassi, E. Žagar, Size characterization and quantification of exosomes by asymmetrical-flow field-flow fractionation, Anal. Chem. 87 (2015) 9225–9233.
[12] J.S. Yang, J.Y. Lee, M.H. Moon, High speed size sorting of subcellular organelles by flow field-flow fractioantion, Anal. Chem. 87 (2015) 6342–6348.
[13] T. Ibrahim, S. Battu, J. Cook-Moreau, P.J. Cardot, Instrumentation of hollow fiber flow field flow fractionation for selective cell elution, J. Chromatogr. B 901 (2012) 59–66.
[14] H. Lee, S.K. Williams, K.L. Wahl, N.B. Valentine, Analysis of whole bacterial cells by flow field-flow fractionation and matrix-assisted laser desorption/ionization time-of-flight mass spectrometry, Anal. Chem. 75 (2003) 2746–2752.
[15] A. Citkowicz, H. Petry, R.N. Harkins, O. Ast, L. Cashion, C. Goldmann, P. Bringmann, K. Plummer, B.R. Larsen, Characterization of virus-like particle assembly for DNA delivery using asymmetrical flow field-flow fractionation and light scattering, Anal. Biochem. 376 (2008) 163–172.
[16] M. Van Bruijnsvoort, K.-G. Wahlund, G. Nilsson, W.T. Kok, Retention behaviour of amylopectins in asymmetrical flow field-flow fractionation studied by multi-angle light scattering detection, J. Chromatogr. A 925 (2001) 171–182.
[17] S. Woo, J.Y. Lee, W. Choi, M.H. Moon, Characterization of Ultrahigh Molecular Weight Cationic Polyacrylamide by Frit-Inlet Asymmetrical Flow Field-Flow Fractionation and Multiangle Lightscattering, J. Chromatogr. A 1429 (2016) 304–310.
[18] J.C. Giddings, F.J. Yang, M.N. Myers, Theroretical and experimental characterization of flow field-flow fractionation, Anal. Chem. 48 (1976) 1126–1132.
[19] M.H. Moon, D. Kang, I. Hwang, P.S. Williams, Field and Flow Programming in Frit-Inlet Asymmetrical Flow Field-Flow Fractionation, J. Chromatogr. A 955 (2002) 263–272.
[20] M.H. Moon, I. Hwang, Hydrodynamic relaxation vs. Focusing/Relaxation in asymmetrical flow field-flow fractionation, J. Liq. Chromatogr. Relat. Technol. 24 (2001) 3069–3083.
[21] K.A. Selting, G.K. Ogilvie, S.E. Lana, M.J. Fettman, K.L. Mitchener, R.A. Hansen, K.L. Richardson, J.A. Walton, M.A. Scherk, Serum alpha 1–Acid glycoprotein concentrations in healthy and tumor-bearing cats, J. Vet. Intern. Med. 14 (2000) 503–506.
[22] M.R. Ajmal, A.S. Abdelhameed, P. Alam, R.H. Khan, Interaction of new kinase inhibitors cabozantinib and tofacitinib with human serum alpha-1 acid glycoprotein. A comprehensive spectroscopic and molecular Docking approach, Spectrochim. Acta Part A Mol. Biomol. Spect. 159 (2016) 199–208.

Journal of Chromatography A, 1591 (2019) 178

Contents lists available at ScienceDirect

Journal of Chromatography A

journal homepage: www.elsevier.com/locate/chroma

Corrigendum

Corrigendum to "Flow optimisations with increased channel thickness in asymmetrical flow field-flow fractionation" [J. Chromatogr. A 1581–1582 (2018) 100–104]

Joon Seon Yang, Myeong Hee Moon*

Department of Chemistry, Yonsei University, 50 Yonsei-ro, Seoul, 03722, Republic of Korea

The author would like to highlight about a mistake in Equations.
There are two places (Eqs. (3) and (6)) in the manuscript.

1) In Eq. (3)

$$t_r = \frac{\pi\eta w^2 d}{2kTbL}\frac{\dot{V}_c}{\dot{V}}$$

Should be corrected with

$$t_r = \frac{\pi\eta w^2 d}{2kT}\frac{\dot{V}_c}{\dot{V}}$$

2) Eq. (6)

$$t_r = \frac{\pi\eta w^2 d}{2kTbL}\frac{\dot{V}_c}{\dot{V}_{eff}}$$

Should be corrected with

$$t_r = \frac{\pi\eta w^2 d}{2kT}\frac{\dot{V}_c}{\dot{V}_{eff}}$$

The authors would like to apologise for any inconvenience caused.

DOI of original article: https://doi.org/10.1016/j.chroma.2018.10.053.
* Corresponding author.
E-mail address: mhmoon@yonsei.ac.kr (M.H. Moon).

https://doi.org/10.1016/j.chroma.2019.03.013